

# MONITORING HURRICANE EFFECTS ON AQUIFER SALINITY USING ALSM

**Michael Starek**

**Ali Sedighi**

PhD Students

Department of Civil and Coastal Engineering

Geosensing Systems Engineering

University of Florida; PO Box 116130; Gainesville, FL 32611

[mstarek@ufl.edu](mailto:mstarek@ufl.edu)

[alised@ufl.edu](mailto:alised@ufl.edu)

## ABSTRACT

During the Atlantic hurricane season of 2004, the Florida Pan Handle, Gulf Coast region, was impacted directly by three hurricanes within approximately a one-month time period. The short temporal span between impacts coupled with the severity of the storms resulted in drastic changes to the littoral zone geomorphology including extensive shoreline erosion and accretion that directly affected the subsurface hydrogeologic environment. The most important direct physical effects of a hurricane are the following: coastal erosion, shoreline inundation owing to higher than normal tide levels plus increased temporary surge levels during storms, and saltwater intrusion primarily into estuaries and groundwater aquifers. Erosion and deposition during the hurricane change the elevation, which causes change in the position of shoreline. The purpose of this study was to investigate the effects of sea level inundation due to the hurricanes on the near shore subsurface freshwater-saltwater interface. By utilizing high-resolution Airborne Laser Swath Mapping (ALSM) altimetry data acquired shortly before and after the three major hurricane landfalls, the change in shoreline topography was estimated to determine both small-scale and large-scale horizontal encroachment and volumetric change in shoreline. This information was used to develop a before and after variable density groundwater flow model to determine the impact of the hurricanes on the subsurface saltwater-freshwater interface. SEAWAT (Langevin 2001; Guo and Langevin 2002), which simulates three-dimensional, variable-density groundwater flow following a modular structure similar to MODFLOW (McDonald and Harbaugh 1988), was selected to represent the saltwater-freshwater interface in this investigation.

## INTRODUCTION

In coastal areas, the position of shoreline is a controlling factor on the saltwater-freshwater interface and the quality of the discharged ground water in a nearby well. In coastal aquifers, a layer of freshwater floats on top of the denser saltwater. The saltwater generally forms a wedge such that the farther inland, the farther below ground is the boundary between fresh and saltwater. When sea level advancement results in a landward movement of the shoreline, the boundary moves inland as well. Because the level of the water table is itself determined by sea level, a retreat in shoreline causes the freshwater-saltwater boundary to rise/advance. The landward and upward shift of this boundary implies that certain freshwater wells may become salty (Titus and Barth 1984), figure 1 below. Hurricanes also introduce saltwater to surficial aquifers by infiltration through inundation caused by high waves and tidal surge (Anderson and Evan 2001). However, only effects due to shoreline encroachment will be investigated herein.

Direct measurement of shoreline change over large distances is technically difficult and too expensive to be feasible at more than a few point locations. However, Airborne Laser Swath Mapping (ALSM) altimetry data commonly referred to as Light Detection and Ranging (LiDAR) can be used to effectively estimate change in elevation from erosion and accretion, and thus change in position of the shoreline can be determined. These data can then be used in a numerical variable density groundwater flow model such as the USGS variable-density code SEAWAT (Guo and Langevin 2002), to monitor the hurricane effects on aquifer salinity.

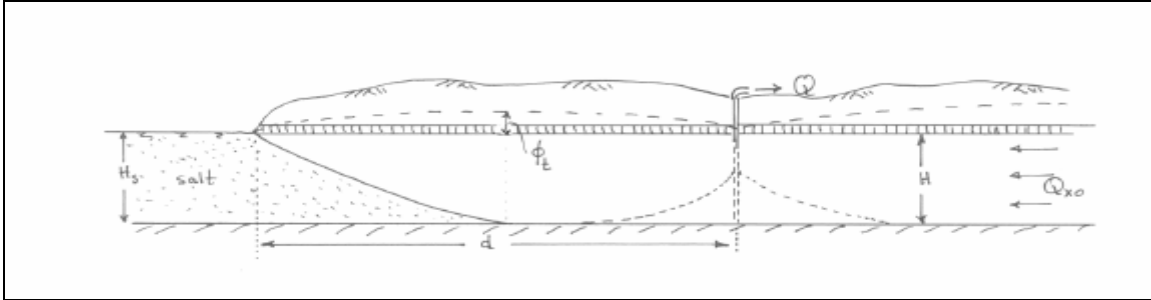


**Figure 1.** Vertical section over a confined aquifer with a well at a distance  $d$  from the coast. The salty seawater is encroaching into the well.

Since there is a direct relationship between shoreline encroachment and increased potential for saltwater infiltration, it is important to model and understand how this interface changes to approximate necessary reductions in pumping rates due to hurricane impact for prevention of saltwater intrusion. Furthermore, dependent to this analysis is the need to quantify the horizontal and volumetric change in shoreline, which will provide insight into the extent and severity of shoreline erosion and accretion caused by the hurricanes to the area of study.

During the Atlantic hurricane season of 2004, the Florida Pan Handle, Gulf Coast region, was impacted directly by hurricanes Francis, Ivan, and Jeanne within approximately the one month time period of September (Figure 2). The short temporal span between impacts coupled with the sudden increase in wave energy delivered to the coast resulted in drastic changes to the littoral zone geomorphology including extensive shoreline erosion and accretion that directly affected the subsurface hydrogeologic environment. The purpose of this study was to investigate the effects of sea level inundation due to the hurricanes on the near shore subsurface freshwater-saltwater interface. By utilizing high-resolution ALSM collected by the University of Florida's Geosensing Engineering and Mapping (GEM) Center shortly before and after the three major hurricane landfalls, the change in shoreline topography will be estimated to determine both small-scale and large-scale horizontal encroachment and volumetric change in shoreline. This information will then be used to develop a before and after variable density groundwater flow model to determine the impact of the hurricanes on the subsurface saltwater-freshwater interface.



**Figure 2.** Storm tracks for hurricane Francis, Ivan, and Jeanne [image courtesy of NOAA Coastal Services Center].  
Note: Ivan had two separate storm events associated with its life cycle as seen above entering the Gulf twice.

## BACKGROUND

### ALSM for Estimating Shoreline Change

The application of ALSM data for topographic mapping of the littoral zone is becoming increasingly important. Neuenchwander et. al. (2000) used an airborne laser altimetry system to map the Kennedy Space Center complex, Florida, for development of a high-resolution digital elevation model (DEM). Before extraction of the “bald-earth” DEM, the data had to be geometrically corrected for inter-flightline biases and cross-track artifacts and the vegetation signature removed. Their results found that the small footprint of the airborne laser data coupled with the potential to acquire multiple returns provides the potential to obtain more accurate, higher-resolution digital elevation models critical for applications such as hydrology and shoreline mapping.

Devine and Mehta (1999) investigated the change of inlet ebb deltas due to severe sea conditions. They explained the potential use of rapid-pre and post-storm surveying for change detection of flood and ebb deltas using an ALSM system to corroborate their analytical time-dependent study.

Tebbens et. al. (2002) investigated shoreline change over a one-year period on the Outer Banks, North Carolina using wavelet analysis and ALSM data collected by NASA’s Airborne Topographic Mapper (ATM). They measured shoreline change by determining the horizontal change in position of the 0.8-m contour sampled from shore-perpendicular profiles spaced at 20-m intervals along the coast. The profiles were obtained from two separate surveys performed in September 1997 and September 1998. The 0.8-m contour interval was taken as the shoreline since the highest tide never exceeded 0.76 m above mean sea level during data collection. The difference in distance of the profiles between the two years yielded the horizontal change in shoreline position.

Woolard et. al. (2003) collected airborne laser data from three different commercial systems to delineate the shoreline at Shilshole Bay, Washington. The Airborne Laser Terrain Mapper (ALTM) and the Scanning Hydrographic Operational Airborne LiDAR Survey (SHOALS) systems developed by Optech, Inc., of Toronto, Canada were used along with the Laser Airborne Depth Sounder (LADS) Mark II, developed to support the royal Australian Navy. The relative differences in results between the systems were compared as well as differences in elevations to those obtained by National Oceanic and Atmospheric Administration (NOAA) multibeam sounding data. To delineate the shoreline a static ground GPS survey was conducted to obtain ellipsoidal information to the closest tidal benchmark to the project area. This allowed the tidal measurements, heights above Mean High Water (MHW) and Mean Lower Low Water (MLLW), to be related to the ellipsoid and provided an elevation correction to bring all the airborne laser datasets to a common vertical datum. MHL and MLLW shoreline vectors (contours) were then extracted from the different datasets.

### Representation of Saltwater-Freshwater Interface in Groundwater Models

In many parts of Florida, saltwater occurs in the upper and lower zones of the Floridian aquifer system near coastal areas. The transition zone between freshwater and saltwater, which is the region over which the chloride concentration changes from approximately 25 mg/L in the freshwater zone to as much as 19,000 mg/L in the saltwater zone, may be relatively narrow in some areas and relatively wide in other areas (Ryder 1985). For example, the transition zone is about 2 miles wide in Hillsborough County and about 30 miles wide in De Soto and Charlotte counties.

In many of the groundwater flow models for these areas in Florida (e.g., Bush and Johnston 1988), the saltwater zone is represented by inactive cells, the freshwater zone is represented by active cells, and the transition zone between freshwater and saltwater is represented by a no-flow boundary. The location of the no-flow boundary may be determined based on predevelopment (e.g., Ryder 1985) or present conditions (Motz and Dogan 2004 and Sepulveda 2002). The interface has been variously assumed to occur at the location of a chloride concentration of 5,000 mg/L (Motz and Dogan 2004 and Sepulveda 2002), 10,000 mg/L (Bush and Johnston 1988), and 19,000 mg/L (Ryder 1985). In these groundwater flow model applications, the location of the no-flow boundary is not changed in response to increased pumping that is projected to occur in the future. Thus, it is assumed that the saltwater-freshwater interface does not move in response to pumping and that pumping impacts do not extend from the freshwater zone to the saltwater zone across the interface. Alternatively, in other groundwater flow models, the freshwater-saltwater interface is represented by a general-head boundary condition (e.g., Guvanansen et al. 2000 and McGurk and Presley 2002). In these applications, it is assumed that the transition zone is represented by a head-dependent flux from the saltwater zone to the freshwater zone and that pumping impacts extend across the interface from the freshwater to the saltwater zone.

The present practice in many groundwater models of assuming a no-flow boundary to represent the saltwater-freshwater interface is conservative in one sense in that calculated drawdowns in the freshwater zone are maximized

by the presence of the no-flow boundary. On the other hand, assuming that a no-flow boundary is present ignores drawdowns that extend into the saltwater zone and also may ignore the potential movement of the interface farther inland into a freshwater zone. Thus, the head-dependent flux associated with the general-head boundary condition may represent better the decrease in head in the freshwater zone and the flow associated with the movement of the interface (Motz and Sedighi 2004).

## DATA SET AND STUDY AREA

The University of Florida’s Geosensing and Engineering Mapping Center (GEM) collected airborne laser data along the shorelines of Bay County, Florida in the Panhandle region shortly before (August) and after (October) the September 2004 hurricanes. The “before” and “after” data sets ((Figure 3) were collected at low tide using an Optech ALTM 2033 system that samples at 33khz (refer to Table 1). The processed data consisted of raw last-return x,y,z-values. The Inlet Beach (Phillips Inlet) and surrounding barrier island region was selected as the representative area of study. This area exhibited large-scale changes due to hurricane impact both along the beach and inlet zone (Figure 3).

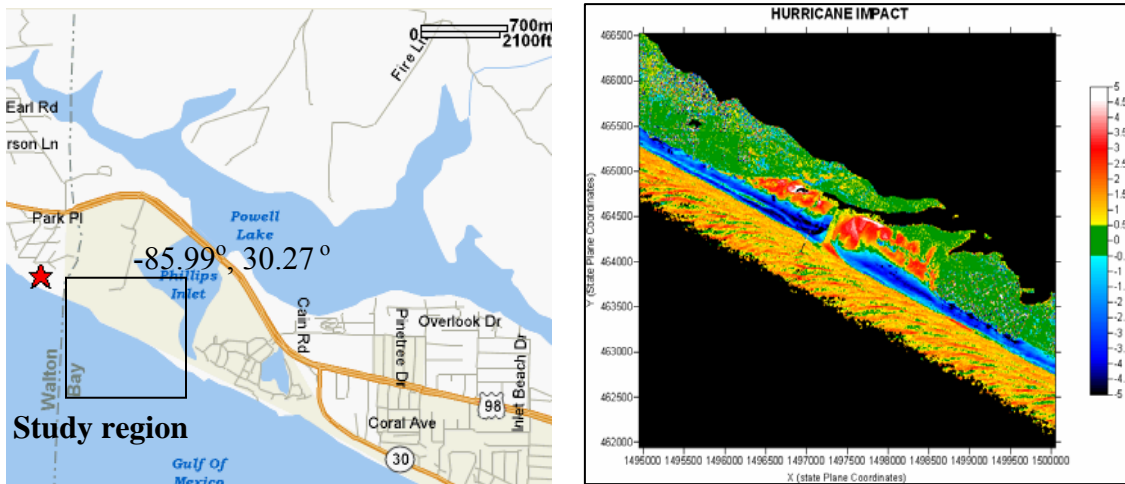


**Figure 3.** Phillips Inlet study area (left); Difference of “Before” and “After” elevation grids showing elevation change in study region after the hurricanes (right).

**Table 1.** UF’s Nominal ALSM Survey Parameters

Flying Speed (ft/s)	Scan Spacing (ft)	Pulse Rate (p/sec)	
200		6.9	33333.0
Indicated Air Speed (nm/h)	Scan Width (f)	Pulses Per Scan	
116.6		1433	595.2
Scan Rate (+/- degrees)	Scan Angle (d)	Distance Between Points Along Scan(ft)	
28.0		20.0	2.4
Flying Height (feet AGL)	Flight line Spacing (ft)	Swath Overlap (ft)	
2000	300		1133

## DETERMINING SHORELINE CHANGE

### Coordinate System Transform

The raw coordinates were processed with respect to the NAD83 datum and projected to Universal Transverse Mercator, Zone 16, meters. The ellipsoid heights were transformed with respect to the NAVD88 vertical datum. The elevations could then be referenced to local tidal datums (i.e. sea level) thereby allowing the determination of a reference contour.

Since the surveys were conducted around low tide, the Mean High Water (MHW) level was selected as the representative shoreline contour. However, to obtain this contour the ALSM data had to be referenced to the MHW tidal datum. To do this, a tidal datum offset had to be determined. The nearest NOAA tidal gauge station was selected as the reference for computation of the tidal offset. At this location, MHW is ~0.395m above Mean Lower Low Water (MLLW). The NAVD88 datum is offset by 0.170 m from MLLW. Since the ALSM elevations are referenced to this datum, the 0.170 m offset was added to the MHW offset to determine a MHL level for the ALSM data. This contour approximately equaled 0.6m and was selected as the proxy for shoreline since collections occurred during approximate low-tide conditions. In addition, elevation biases between the two flights due to systematic errors in the laser system were removed by taking an along-road elevation profile and correcting for biases between the two flights.

### Separation of Beach and Dunes

The non-filtered before and after data were gridded to 1-m digital elevation models (DEMs) using ordinary kriging and the commercial software package *Surfer*. Each grid was formed using a linear variogram model and a nugget effect with error variance set to 0.07m. This error represents the uncertainty in UF's ALSM system, which is approximately equal to 7 cm vertical. The micro variance was set to 0. The following is a brief explanation of the error variance and micro variance nugget effect parameters:

The *Error Variance* is a measure of the direct repeatability of the data measurements. The *Error Variance* values take these variances in measurement into account. A non-zero *Error Variance* means that a particular observed value is not necessarily the exact value of the location. The *Micro Variance* is a measure of variation that occurs at separation distances of less than the typical nearest neighbor sample spacing. The *Micro Variance* allows you to specify the variance of the small-scale structure (Cressie and Noel 1991).

The gridded 1-m DEMs were imported into *Surfer* and plotted as shaded relief maps to allow determination of a reference polygon for separation of the shoreline zone (beach) points from the non-beach (dunes and landward zone) points. The raw points for the "before" and "after" data sets were separated using the polygon by grouping points within the polygon as non-beach and those outside as beach points. This allowed separate filtering of the beach and non-beach zones. This is necessary because the parameters that work well on the beach for filtering non-ground points generally do not provide satisfactory results for the dunes and landward zones.

### Filtering

The separate regions were then filtered separately to remove vegetation and buildings using a Height Tolerance Filter (HTF) developed by the UF GEM center. The filtering method implemented is based on local height changes, with filter parameters tuned to different land relief and cover types such as flat beaches, dunes, and canopied areas. It utilizes the following parameters:

[ Floor Ceiling Segment\_Length Width Height\_tolerance]

Floor is a minimum elevation, ceiling is a maximum elevation, segment\_length is set to the maximum length of the structures you are attempting to remove, width is the width of the search cell, and height-tolerance is used to determine whether an elevation jump signals a non-ground point. Since this filter is non-adaptive, it requires significant trial and error, continually testing different parameters. After several trials, the following parameters were found to work best for filtering out non-ground points in the beach and non-beach zones: Beach parameters (m) = [-1.5 20 15.5 1 0.2] and Non-beach parameters (m) = [-1.5 13 20 1 0.2]. Once the data was filtered it was recombined and gridded using an extended variogram search radius that was slightly more than the max segment length to compensate for data voids formed during the filtering process, Figure 4 and 5 below.

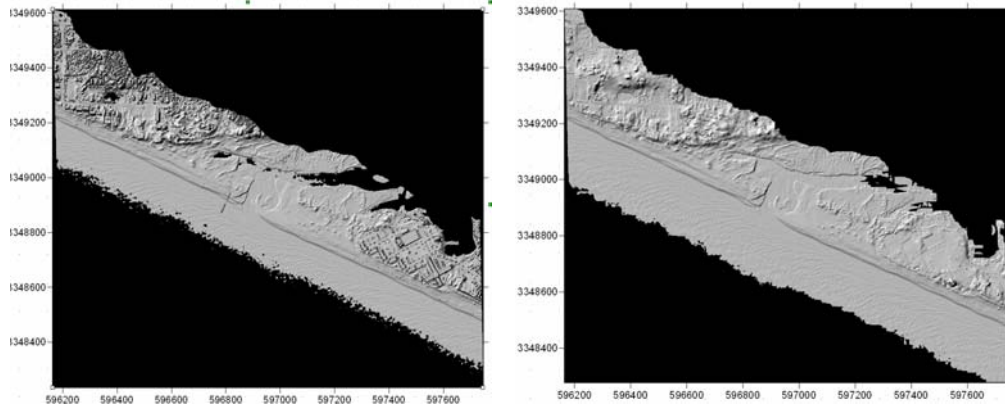


**Figure 4.** “Before” non-filtered and filtered 1-m DEM (x = Easting, y = Northing (m))

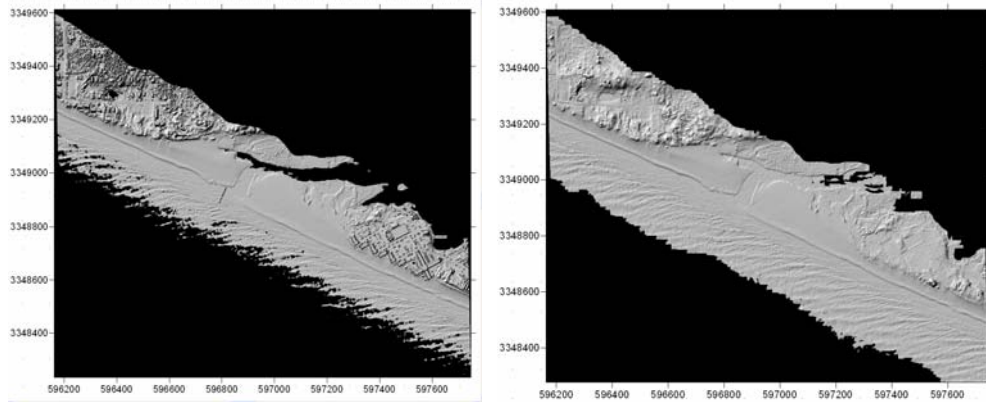


**Figure 5.** “After” non-filtered and filtered 1-m DEM (x = Easting, y = Northing (m)).

### Delineation of Shoreline

The 0.6m contour was extracted using the “before” and “after” filtered 1-m DEMs to represent the shoreline. However, there were additional contours not delineating the shoreline that had to be removed. In *Surfer* a polygon was digitized to exclude all points outside the shoreline zone. This was done for the “before” and “after” grids and the final contours were recomputed as displayed in Figure 6.

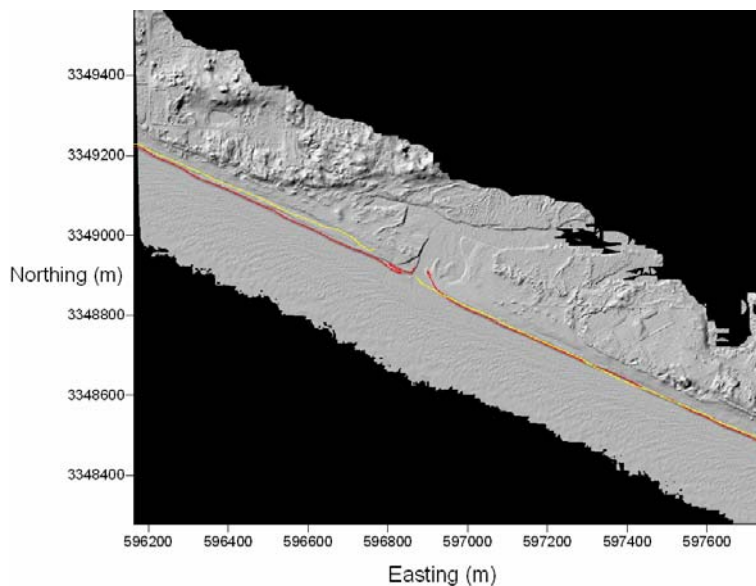


**Figure 6.** Shoreline contours (red is “before”, yellow is “after”).

## Quantification of Shoreline Change

The next step was to determine the relative change in the shoreline signal by determining the change in shore normal profiles between equally spaced points along the shoreline. The before and after filtered grids were imported into the *MatLab* computing environment and a procedure was developed to align the strike of the beach horizontally. The strike of the beach was estimated to be  $-26.5^\circ$  from the horizontal. Using a rotation matrix and bilinear interpolation to resample, the grids were rotated  $-26.5^\circ$  to align the shoreline horizontally, Figure 7 and 8.

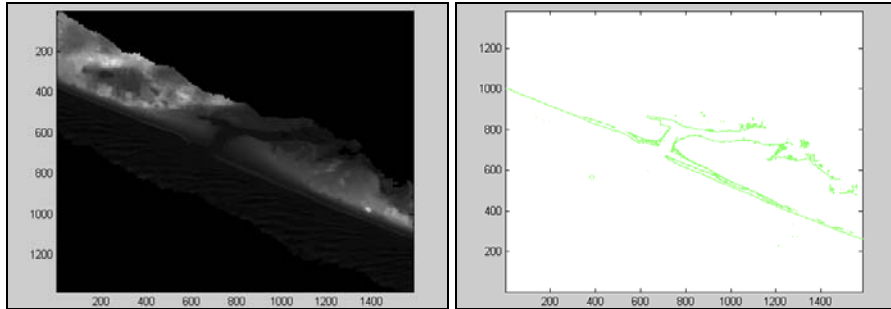


Figure 7. Before rotation.

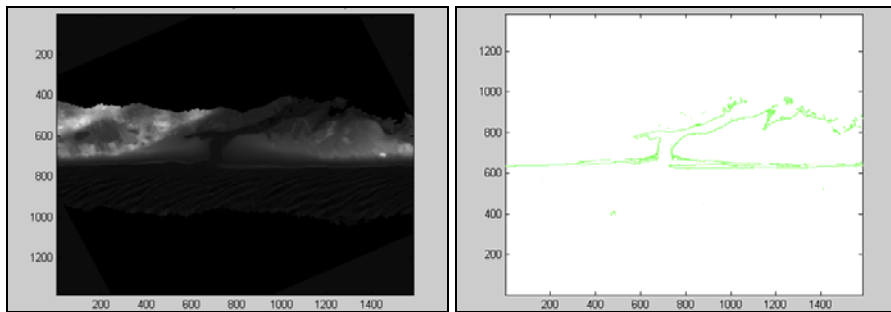


Figure 8. After rotation.

By performing this operation, the shore normal change in profile could now be auto-approximated as the difference in y-direction between the “before” and “after” contour cells. A routine was developed to determine the contour grid cells and then compute the change in shoreline for 10-m sampling frequency. Analysis of the shoreline change indicates that the majority of encroachment and erosion occurred along the west shoreline and within the west side of Phillips inlet, Figure 9 below. Therefore, the west shoreline was selected as the region of interest to develop the groundwater model.

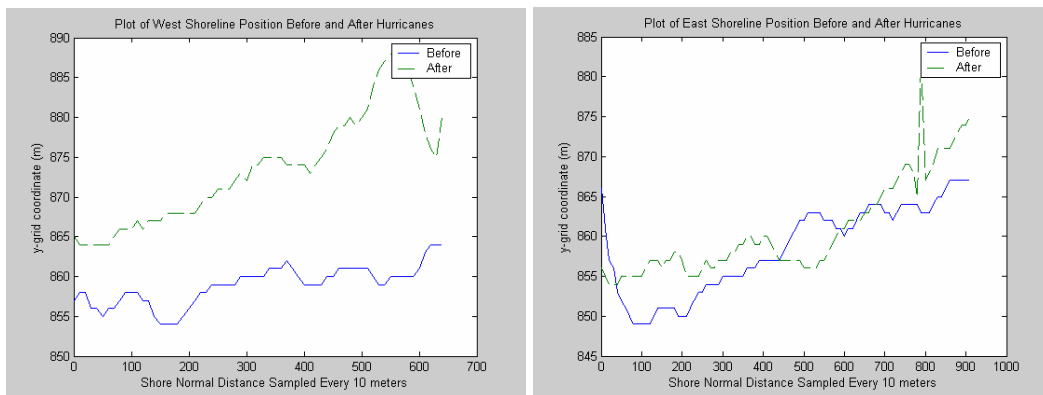


Figure 9. Along-shore profiles showing change due to hurricanes for west (left) and east (right) shoreline. Observe significant encroachment to west shoreline.

The following statistics were determined for 10-m sampling frequency:

**West Shoreline Change Statistics:**

Max Change: 28.0m  
 Median: 14.0m  
 Mean: 14.5m

**East Shoreline Change Statistics:**

Max Change: 19.0m  
 Median: 3.0m  
 Mean: 2.2m

**DEVELOPMENT OF THE GROUNDWATER MODEL FOR WEST SHORELINE**

**Selection of Variable-Density Code**

SEAWAT (Langevin 2001; Guo and Langevin 2002), which simulates three-dimensional, variable-density groundwater flow following a modular structure similar to MODFLOW (McDonald and Harbaugh 1988), was selected to represent the saltwater-freshwater interface in this investigation. The source code for SEAWAT combines MODFLOW with the solute-transport code MT3DMS (Zheng and Wang 1999) into a single program that solves the coupled flow and solute-transport equations. As a result, SEAWAT reads and writes standard MODFLOW and MT3DMS data sets. Several commercially available pre- and post-processors can be used to create input data sets and analyze simulation results, including Groundwater Vistas, Version 4 (Environmental Simulations 2004), which was used in this investigation.

In SEAWAT, the dependent variable is the equivalent freshwater head:

$$h_{fw} = \frac{P_N}{\rho_f g} + Z_N \quad (1)$$

where:  $h_{fw}$  = equivalent freshwater head;  $P_N$  = pressure at point N;  $\rho_f$  = density of freshwater;  $g$  = acceleration due to gravity; and  $Z_N$  = elevation of point N above a datum. The equivalent freshwater head and the head in a saline aquifer are related by:

$$h_{fw} = \frac{\rho}{\rho_f} h - \frac{\rho - \rho_f}{\rho_f} Z \quad (2)$$

And

$$h = \frac{\rho_f}{\rho} h_{fw} + \frac{\rho - \rho_f}{\rho} Z \quad (3)$$

where  $h$  = head; and  $\rho$  = density of saline groundwater at point N.

**Design of Numerical Experiments**

The numerical experiments consisted of obtaining solutions with different boundary conditions based on the shoreline position using SEAWAT. Considering long execution times for three-dimensional models, two-dimensional models were first created to investigate primary results. Both two-dimensional and three-dimensional models were assembled to represent a coastal aquifer.

**Two-Dimensional Cross-Section**

For the before hurricane simulations, a two-dimensional vertical cross-section was discretized into one row, 130 columns, and 40 layers. The columns were equally spaced with  $\Delta x = 5$  m for a total length of 650 m, and the layers were equally spaced with  $\Delta z = 5$  m for a total depth of 200 m. The width of the row perpendicular to the direction of flow in the cross-section was set arbitrarily to  $\Delta y = 5$  m. Boundary conditions in column 1, layers 1-40 are specified head and concentration. The head value is 0 and the concentration at the coastal boundary was specified as constant and equal to  $35 \text{ kg/m}^3$ , representing the total dissolved solids (TDS) concentration of seawater. In the SEAWAT solution, equivalent freshwater heads at the coastal boundary were calculated over the vertical using Equation 2 with  $h = 0$ ,  $\rho = 1,025 \text{ kg/m}^3$ , and  $\rho_f = 1,000 \text{ kg/m}^3$ . Boundary conditions in column 130, layers 1-40 are



specified head = 1 m and concentration is set to zero. For the after hurricane simulations, boundary conditions in columns 2-6, layers 1-40 are added as specified head = 0 and concentration = 35 kg/m<sup>3</sup>.

### Three-Dimensional Model

Based on the simulation results of the two-dimensional vertical cross-section model and the selected representative barrier island, a three-dimensional model was developed. The three-dimensional model consisted of 120 rows, 120 columns, and 20 layers. The rows and columns were equally spaced with  $\Delta y = 5$  m for a total width of 600 m. The layers were equally spaced with  $\Delta z = 5$  m for a total depth of 100 m. The “before” hurricane shoreline map was imported to the model to determine the boundary conditions, inactive cells in the south part of the model were assigned a head value and concentration. The head value is 0 and the concentration at the coastal boundary was specified as constant and equal to 35 kg/m<sup>3</sup>, representing the total dissolved solids (TDS) concentration of seawater. In the SEAWAT solution, equivalent freshwater heads at the coastal boundary were calculated over the vertical using Equation 2 with  $h = 0$ ,  $\rho = 1,025$  kg/m<sup>3</sup>, and  $\rho_f = 1,000$  kg/m<sup>3</sup>. Boundary conditions in the north part (row 130), layers 1-20 are specified head = 1 m and concentration is set to zero. For the after hurricane simulations, boundary conditions in the south part was expanded to the north, based on the shoreline map after the hurricane. Six monitoring wells were included in both three-dimensional models to detect the change in concentration in different places of the model. All monitoring wells are extended from layer 1 to layer 20.

### Aquifer Parameters

The boundary conditions for the shoreline, the hydraulic conductivities, and other aquifer parameters (see Table 2) were chosen so that the cross-section was representative of a field-scale coastal aquifer such as the Floridian aquifer system in the southeastern U.S.A.

**Table 2. Aquifer parameters and boundary inflow and head used in the numerical experiments**

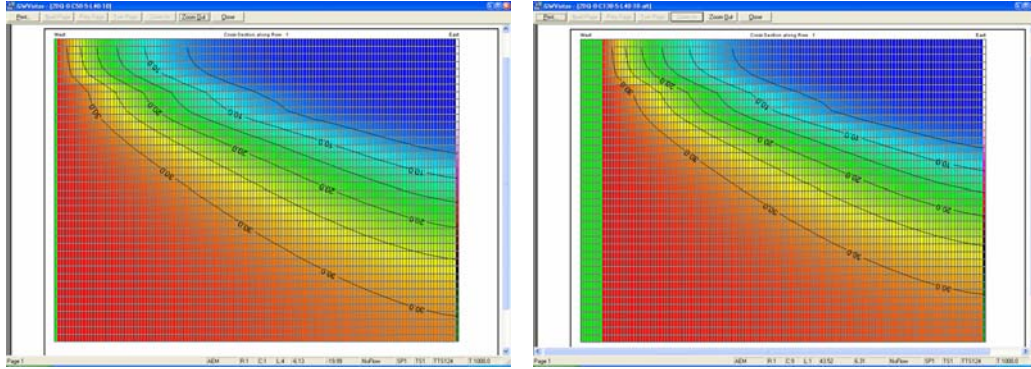
Parameter	Value
Horizontal hydraulic conductivity ( $K_H$ )	50 m/day
Vertical hydraulic conductivity ( $K_V$ )	0.5 m/day
Longitudinal dispersivity ( $\alpha_L$ )	125 m
Transverse dispersivity ( $\alpha_T$ )	12.5
Vertical dispersivity ( $\alpha_V$ )	1.25 m
Porosity ( $n$ )	0.30
Flow per unit width (Q/W) for specified-flux boundary condition	2.0 m <sup>2</sup> /day
Hydraulic head at upstream boundary for specified-head boundary condition	4.95 m

### Solution Scheme

In both the two-dimensional and three-dimensional models, the SEAWAT solutions were obtained using the implicit finite-difference solution scheme and the central-difference weighting technique. The flow part of the solution was run in one time step using a stress period equal to  $1.0 \times 10^3$  days with a closure criterion for the equivalent freshwater heads equal to  $1.0 \times 10^{-9}$  m. In the transport part of the solution, the initial transport time step size was 0.001 days, the time step multiplier was 1.1, and the maximum time step size was 50 days. The generalized conjugate gradient (GCG) solver was used with a specified closure criterion of 0.0001 kg/m<sup>3</sup>. The SEAWAT solutions required 124 transport time steps to reach  $1.0 \times 10^3$  days. Initial values for heads and concentrations were set arbitrarily to zero, and steady-state conditions for heads and concentrations at  $1.0 \times 10^3$  days were verified by plotting hydrographs for heads and concentrations at locations along the bottom of the aquifer where the advancing saltwater-freshwater interface required the longest time to reach an equilibrium location. The MODFLOW solutions were obtained by running MODFLOW to steady-state conditions at  $1.0 \times 10^3$  days in one time step, with a closure criterion for the equivalent freshwater head equal to  $1.0 \times 10^{-9}$  m and the initial heads arbitrarily set equal to zero.

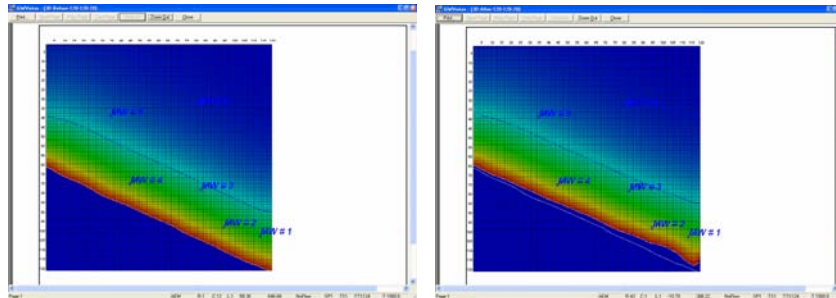
## RESULTS OF NUMERICAL EXPERIMENTS

Figure 10, shows the graphical results of concentration for the two-dimensional models, when the advancing saltwater-freshwater interfaces reach an equilibrium location after 1,000 days.



**Figure 10.** Cross-section TDS concentrations for the two-dimensional models, calculated using SEAWAT.

Figure 11 and 12 show the graphical results of concentration before and after hurricane, when the advancing saltwater-freshwater interfaces reach an equilibrium location. Figure 11 shows a plane view of concentration before and after hurricane and Figure 12 shows concentration change along column 95 where monitoring well number two is located. In all these figures, the red color close to the shoreline indicates high values of concentration and as we go further inland, concentration decreases as expected. From these figures, the change in concentration is clearly visible in the before and after simulations. The equilibrium locations of the advancing saltwater-freshwater interfaces were checked by observing the concentration-time graphs in the monitoring wells.



**Figure 11.** Plane view of TDS concentrations calculated using SEAWAT for before and after hurricane boundary conditions.

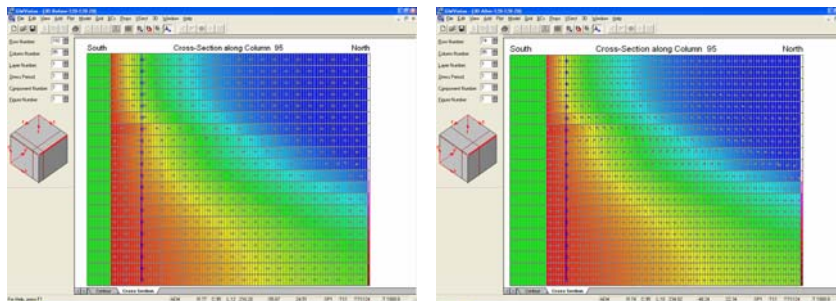


**Figure 12.** Cross-section TDS concentrations along column 95, calculated using SEAWAT for before and after hurricane boundary conditions.

Figure 13 below shows the section profile of concentration vs. distance along column 95 for before and after hurricane in layer one, layer ten, and layer 15. The results show that concentration change happens mostly in the areas closer to the shoreline and as we go further inland, the difference in concentration decreases. Furthermore, concentration change appears mostly in the upper layers of the model.

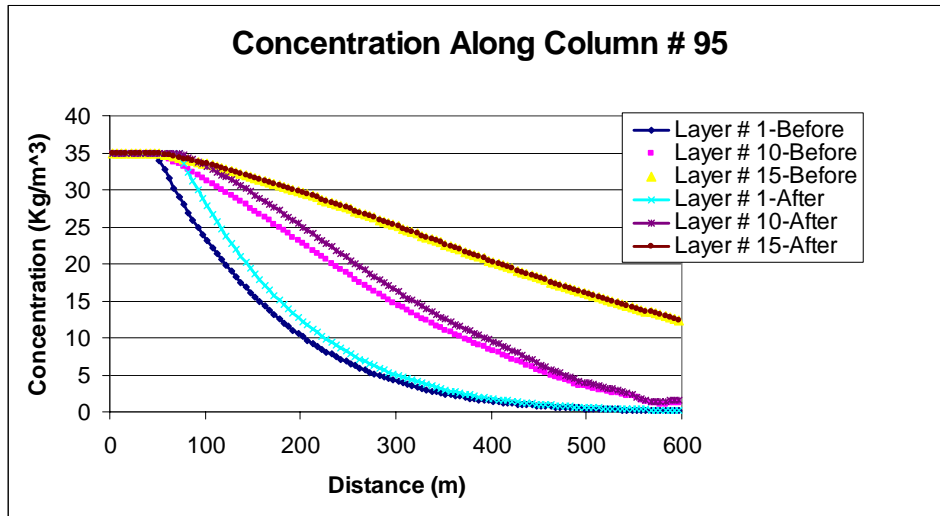


**Figure 13.** Section profile of TDS concentration vs. distance along column 95 for before and after hurricane in layer one, layer ten, and layer 15.

## CONCLUSION

The results from this investigation indicate that the mean encroachment of approximately 14.5m for the west shoreline was significant enough to impact the subsurface freshwater-saltwater interface. The majority of concentration change observed in the numerical model occurs near shore, and as expected, the further inland the less prominent was the observed change. Additionally, concentration change appears mostly in the upper layers of the model.

The results obtained in this investigation are based on two- and three-dimensional models that are intended to be representative of actual but greatly simplified, hydrogeologic conditions. Other representations, such as multiple aquifers and different upstream boundary conditions, could be investigated. For example, models with two or more confined aquifers and a water-table aquifer could be tested, and general-head boundary conditions could be specified at the upstream freshwater boundary instead of specified-head conditions. Also, existing concentration values in data collection sites are required to validate the results obtain in this study. Another important issue is the assumption that equilibrium conditions relative to saltwater intrusion exist. The model could be developed for transient conditions with multiple stress periods to investigate the change in concentration in shorter periods of time. The importance of non-equilibrium conditions relative to sea-level changes that may be occurring in regional aquifer systems also needs to be better understood.

## REFERENCES

- Anderson, Jr. William P., and D.G. Evans. 2001. *Saltwater intrusion from above - Aquifer salinization from storm overwash*. Symposium: Groundwater Conditions in Coastal Aquifer Systems: Past, Present, and Future. GSA Abstracts with Programs 33(2).
- Barth, M.C. and J.G. Titus (eds). 1984. *Planning for Sea Level Rise Before and After a Coastal Disaster*. Van Nostrand Reinhold, New York.
- Bush, P.W., and R.H. Johnston. 1988. *Ground-Water Hydraulics, Regional Flow, and Ground-Water Development of the Floridan Aquifer System in Florida and in parts of Georgia, South Carolina, and Alabama*. Professional Paper 1403-C. Washington, D.C.: U.S. Geological Survey.
- Cressie and Noel. 1991. *Statistics for Spatial Data*, John Wiley and Sons, New York, from *Surfer* reference.
- Devine, P. and A. Mehta, 1999. *Modulation of Microtidal Inlet Ebb Deltas By Severe Sea*. Coastal Sediments '99. Vol. 2, ASCE, Reston, VA.
- Guo, W., and C.D. Langevin. 2002. *User's Guide to SEAWAT: a Computer Program for Simulation of Three-Dimensional Variable-Density Ground-Water Flow*. Open-File Report 01-434. Tallahassee, Fla.: U.S. Geological Survey.
- Guvanansen, V., S.C. Wade, and M.D. Barcelo. 2000. Simulation of regional ground water flow and salt water intrusion in Hernando County, Florida. *J. Ground Water* 38(5):772-783, September-October.
- Handcock and Stein. 1993. *A Bayesian Analysis of Kriging*. Technometrics, Vol.35, No.4, Nov. 1993.
- McDonald, M.G., and A.W. Harbaugh. 1988. *A Modular Three-Dimensional Finite-Difference Ground-Water Flow Model*. Techniques of Water Resources Investigations Report. Book 6, Chapter A1. Washington, D.C.: U.S. Geological Survey.
- McGurk, B., and P. Presley. 2002. *Simulation of the Effects of Groundwater Withdrawals on the Floridan Aquifer System in East-Central Florida: Model Expansion and Revision*. Technical Publication SJ2003-3. 196 pp. Palatka, Fla.: St. Johns River Water Management District.
- Motz, L.H., and A. Dogan. 2004. *North-Central Florida Active Water-Table Regional Groundwater Flow Model (Final Report)*. Palatka, Fla.: St. Johns River Water Management District.
- Motz, L.H., and A. Sedighi. 2004. Investigating the impacts of pumping on the saltwater zone in a groundwater aquifer. (Draft) Final Report. Palatka, Florida: St. Johns River Water Management District.
- Neuenschwander, A., M. Crawford, C. Weed, and R. Gutierrez. 2000. *Extraction of Digital Elevation Models for Airborne Laser Terrain Mapping Data*. IEEE: Geoscience and Remote Sensing Symposium 2000.
- Ryder, P.D. 1985. *Hydrology of the Floridan Aquifer System in West-Central Florida*. Professional Paper 1403-F. 63 pp. Washington, D.C.: U.S. Geological Survey.
- Sepulveda, N. 2002. *Simulation of Ground-Water Flow in the Intermediate and Floridan Aquifer Systems in Peninsula Central Florida*. Water Resources Investigations Report 02-4009. 130 pp. Tallahassee, Fla.: U.S. Geological Survey.
- Tebbens, S., S.M. Burroughs, and E. Nelson. 2002. *Wavelet analysis of shoreline change on the Outer Banks of North Carolina: An example of complexity in the Marine Sciences*. National Academy of Sciences Colloquium: Self-organized Complexity in the Physical, Biological, and Social Sciences, March 23-24, 2001.
- Woolard et. al., 2003. *Shoreline Mapping from Airborne LiDAR in Shilshole Bay, Washington*. NOAA and NOS.
- Zheng, C., and P.P. Wang. 1999. *MT3DMS: A Modular Three-Dimensional Multispecies Transport Model for Simulation of Advection, Dispersion, and Chemical Reactions of Contaminants in Groundwater Systems; Documentation and User's Guide*. Contract Report SERDP-99-1. Washington, D.C.: U.S. Army Corps of Engineers.